49th IEEE Conference on Decision and Control
December 15-17, 2010
Hilton Atlanta Hotel, Atlanta, GA, USA

Dynamics exploration of a single-track rigid car model with load transfer

Alessandro Rucco Giuseppe Notarstefano John Hauser

Abstract— **In this paper we explore the dynamics of a single-track car model. We develop a model of a rigid car inspired to the well known bicycle model. The bicycle model is a planar rigid model that approximates the vehicle as a rigid body with two wheels. However, the bicycle model does not allow to describe the effect of load transfer, since it does not model the suspensions. Using an explicit formulation of the holonomic constraints imposed on the rigid model, we are able to model the load transfer of the car. The resulting model can be seen as a limit condition of a model with suspensions whose stiffness goes to infinity. The load transfer allows to have a more accurate model for the tires. We use a standard model known as Pacejka model that provides empirical curves describing the forces generated by the tires. With this model in hand, we perform an analysis of the equilibrium manifold of the vehicle and, as main contribution of the paper, we explore the trajectories of the system by use of novel nonlinear optimal control techniques. These techniques allow us to compute aggressive trajectories of the car vehicle and study how the vehicle behaves depending on its parameters. We compute trajectories for the vehicle on a real car testing track.**

I. Introduction

A new emerging concept in car design and development is the use of *virtual cars*, i.e., software tools that reproduce the behavior of the real vehicle with high fidelity. This allows to perform dynamic tests before developing the real prototype, thus reducing costs and time to market. This engineering area is called *virtual prototyping*.

Many models have been introduced in the literature to describe the motion of a car vehicle both for simulation and control. Starting from the simplified bicycle model models of different complexity can be designed that include some of the car subsystems such as the transmission system, the differential and the engine [1], [4], [5], [13]. In order to explore the dynamic capabilities of a car vehicle or to design control strategies to drive it, it is necessary to identify dynamic models that capture interesting dynamic behaviors and, at the same time, can be described by ordinary differential equations of reasonable complexity. The bicycle model is a planar rigid model that approximates the vehicle as a rigid body with two wheels. It is widely used in the literature since it captures many interesting phenomena with few tractable equations. However, this model does not capture some important dynamic effects. One of them is load transfer. The inclusion of suitable holonomic constraints allows us to add this phenomenon to the rigid bicycle model with a reasonable increase in the model complexity. This mathematical idea was proposed for a rigid motorcycle model in [9], [12].

The contributions of the paper are as follows. We develop a model of a rigid car that is inspired to the well known bicycle model. Using an explicit formulation of the holonomic constraints imposed on the rigid model, we are able to model the load transfer of the car. The resulting model can be seen as a limit condition of a model with suspensions whose stiffness goes to infinity. Load transfer allows to have a more accurate model for the tires. In particular, we use a standard model known as Pacejka model, [3], [6], that provides empirical curves describing the forces generated by the tires. With this model in hand, we perform an analysis of the equilibrium manifold of the vehicle, namely we study trajectories of the system that can be performed by use of constant inputs. By means of suitable zero finding techniques combined with continuation methods, we compute the equilibrium manifold and parametrize it with respect to the lateral acceleration and the velocity of the vehicle. A comparison is performed between a standard car and a sport car. Finally, we explore the trajectories of the system by use of novel nonlinear optimal control techniques introduced in [10]. These techniques allow to compute trajectories of a nonlinear system that minimize a desired cost functional. In particular, it is possible to compute trajectories of the system (curves satisfying the dynamics) that are "close" to an assigned curve (chosen on the basis of a desired objective behavior). Using these techniques we are able to compute aggressive trajectories of the car vehicle and study the vehicle performance depending on its parameters. We show a set of test maneuvers, in particular we compute trajectories for the vehicle on an aggressive turn of a real car testing track.

The rest of the paper is organized as follows. In Section II we introduce and develop the car model. In Section III we characterize the equilibrium manifold of the car and provide a comparison between two significant choices of the car parameters. Finally, in Section IV we describe the strategy for trajectory exploration and provide numerical computations performed on a real racing track.

II. Rigid car model development

In this section we introduce the car model studied in the paper. The car model consists of a single planar rigid body that interacts with the road at two body-fixed contact points. The center of mass and the two contact points all lie within a plane with the center of mass located at distance b from the rear contact point and a from the front one, respectively. Each contact-point/road-plane interaction is modeled using a *Pacejka Magic Formula* tire model [3]. The body-frame of

Alessandro Rucco and Giuseppe Notarstefano are with the Dipartimento di Ingegneria dell'Innovazione, Università del Salento, Via per Monteroni, 73100 Lecce, Italy, {alessandro.rucco, giuseppe.notarstefano}@unisalento.it

John Hauser is with the Department of Electrical and Computer Engineering, University of Colorado, Boulder, CO 80309-0425, USA, hauser@colorado.edu

978-1-4244-7746-3/10/$26.00 ©2010 IEEE

the car is attached at the rear contact point with x-y-z axes oriented in a forward-right-down fashion. We let $\mathbf{x} \in \mathbb{R}^3$ and $R \in SO(3)$ denote the position and orientation of the frame with respect to a fixed spatial-frame with x-y-z axes oriented in a north-east-down fashion. R maps vectors in the body frame to vectors in the spatial frame so that, for instance, the spatial angular velocity ω^s and the body angular velocity ω^b are related by $\omega^s = R\omega^b$ and $\omega^b = R^T\omega^s$. Similarly, $\mathbf{x}^s = \mathbf{x} + R\,\mathbf{x}^b$ gives the spatial coordinates of a point on the body with body coordinates $\mathbf{x}^b \in \mathbb{R}^3$. The orientation R of the (unconstrained) rigid car model can be parameterized (using Roll-Pitch-Yaw parametrization) as follows

$$R(\psi,\theta) = R_z(\psi)R_y(\theta) = \begin{bmatrix} c_\psi c_\theta & -s_\psi & c_\psi s_\theta \\ s_\psi c_\theta & c_\theta & s_\psi s_\theta \\ -s_\theta & 0 & c_\theta \end{bmatrix}$$

where θ and ψ are respectively the pitch and yaw angles (we use the notation $c_\psi = \cos(\psi)$, etc.)[1]. The mapping $(\theta;\psi) \mapsto R$ is locally one-to-one (i.e., there are no singularities).

Let x, y and z be the coordinates of the rear contact point with respect to the spatial frame. The vector

$$q = (x, y, z, \theta, \psi)^T = (\mathbf{x}, \phi)^T$$

provides a valid set of generalized coordinates for dynamics calculations. A scheme of the rigid car model is shown in Figure 1.

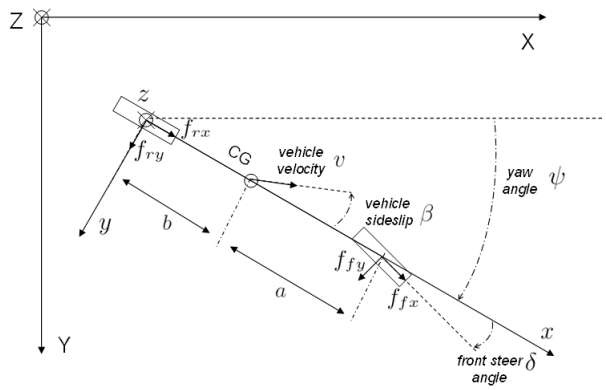

Fig. 1. Single-Track Rigid Car. The figure show the quantities used to describe the model.

A. Contact point constraints and tire model

We constrain the contact points to the road plane. The front and rear contact points coordinated expressed in the body frame are $\mathbf{x}_f^b = (a+b, 0, 0)^T$ and $\mathbf{x}_r^b = (0,0,0)^T$. The coordinates of the rear and front contact points in the spatial frame, respectively $\mathbf{x}_r^s = (x_r^s, y_r^s, z_r^s)$ and $\mathbf{x}_f^s = (x_f^s, y_f^s, z_f^s)$, are $\mathbf{x}_r^s = \mathbf{x}$ and $\mathbf{x}_f^s = \mathbf{x} + R\,\mathbf{x}_f^b$ so that the velocities are given by $v_r^s = \dot{x}$ and

$$\begin{aligned} v_f^s &= \dot{\mathbf{x}} + R\,\hat{\omega}^b\mathbf{x}_f^b \\ &= \dot{\mathbf{x}} + R\,\omega^b \times \mathbf{x}_f^b \\ &= \dot{\mathbf{x}} - R\,\mathbf{x}_f^b \times \omega^b \\ &= \dot{\mathbf{x}} - R\,\hat{\mathbf{x}}_f^b J_{\omega^b}(\phi)\dot{\phi}, \end{aligned}$$

[1]We neglect the roll motion of the car.

where $\hat{\omega}^b$ is the skew-symmetric matrix associated to the angular velocity ω^b and J_{ω^b} is the Jacobian mapping $\dot{\phi}$ to ω^b. Next, we impose the constraint that the rear and front contact points have zero velocity along the z axis. The velocities are given by $\dot{z}_r = \dot{z}$ and

$$\dot{z}_f = \dot{z} - e_3^T R\,\hat{\mathbf{x}}_f^b J_{\omega^b}(\phi)\dot{\phi} = J_{\dot{z}_f}(\phi)\dot{q},$$

where z_f is the position of the front contact point. The front and rear constraints may be written in the form $A(q)\dot{q}$=0, where

$$A(q) = \begin{bmatrix} J_{\dot{z}_f}(\phi) \\ J_{\dot{z}_r}(\phi) \end{bmatrix} = \begin{bmatrix} 0 & 0 & 1 & -(a+b)c_\theta & 0 \\ 0 & 0 & 1 & 0 & 0 \end{bmatrix}. \quad (1)$$

The vector $\lambda = [f_{fz}\ f_{rz}]^T \in \mathbb{R}^2$ gives the constraint (normal) forces so that $A^T(q)\lambda$ is the vector of generalized constraint forces.

With the above expression for the normal forces in hand, we can introduce the models of the tire forces by using a suitable version of the Pacejka's Magic Formula [3], [7]. Before, we clarify our notation. We use a subscript "f" ("r") for quantities of the front (rear) tire. When we want to give a generic expression that holds both for the front and the rear tire we just suppress the subscript. Thus, for example, we denote the generic normal tire force f_z, meaning that we are referring to f_{fz} for the front tire and f_{rz} for the rear one.

We assume that the rear and front forces tangent to the road plane, f_x and f_y, depend linearly on the normal forces, namely $f_{rx} = f_{rz}\mu_{rx}$, etc. . Let κ be the longitudinal slip ratio of the tire and $\tan\beta = v_y/v_x$ where v_x and v_y are the longitudinal and lateral velocities, respectively, at the contact point expressed in the local tire frame. The combined slip formulas are

$$\begin{aligned} f_x &= -f_z\mu_x(\kappa,\beta) = -f_z f_{x0}(\kappa) g_{x\beta}(k,\beta) \\ f_y &= -f_z\mu_y(\kappa,\beta) = -f_z f_{y0}(\beta) g_{yk}(k,\beta), \end{aligned}$$

where the pure longitudinal slip is given by

$$f_{x0}(\kappa) = \mu_x \sin\left[c_x \arctan\left\{b_x\kappa - e_x(b_x\kappa - \arctan b_x\kappa)\right\}\right],$$

the pure lateral slip is given by

$$f_{y0}(\beta) = \mu_y \sin\left[c_y \arctan\left\{b_y\beta - e_y(b_y\beta - \arctan\left(b_y\beta\right))\right\}\right]$$

and the loss functions for combined slips are given by

$$\begin{aligned} g_{x\beta}(\kappa,\beta) &= \cos\left[c_{x\beta} \arctan\left\{\beta \frac{r_{bx1}}{1 + r_{bx2}^2\kappa^2}\right\}\right] \\ g_{yk}(\kappa,\beta) &= \cos\left[c_{yk} \arctan\left\{\kappa \frac{r_{by1}}{1 + r_{by2}^2\beta^2}\right\}\right]. \end{aligned}$$

The values of the parameters used in the paper are provided in Appendix.

The front longitudinal forces expressed in the body frame, f_{fx}^b and f_{fy}^b, are obtained by rotating the forces in the tire frame according to the steering angle δ, so that, e.g.,

$$f_{fx}^b = f_{fx}c_\delta - f_{fy}s_\delta$$

Substituting the above expressions for f_{fx} and f_{fy}, we get

$$\begin{aligned} f_{fx}^b &= -f_{fz}\big(\mu_{fx}(\kappa_f,\beta_f)c_\delta - \mu_{fy}(\kappa_f,\beta_f)s_\delta\big) \\ &:= -f_{fz}\tilde{\mu}_{fx}(\kappa_f,\beta_f,\delta). \end{aligned}$$

In the rest of the paper, abusing notation, we will suppress the 'tilde' and use $\mu_{fx}(\kappa_f, \beta_f, \delta)$ to denote $\tilde{\mu}_{fx}(\kappa_f, \beta_f, \delta)$.

As regards the control inputs, we assume that the front wheel evolves with pure rolling so that we can set $\kappa_f = 0$. Thus, the control inputs of the car turn to be the rear longitudinal slip κ_r and the steering angle δ.

B. Lagrangian dynamics

We now determine the dynamics of the constrained system via the Euler-Lagrange equations. To do this, we define the Lagrangian $\mathcal{L}$ as the difference between the kinetic and potential energies $\mathcal{L}(q, \dot{q}) = T(q, \dot{q}) - V(q)$. The equations of motion for the unconstrained system are given by

$$\frac{d}{dt}\frac{\partial \mathcal{L}}{\partial \dot{q}}^T - \frac{\partial \mathcal{L}}{\partial q}^T = U$$

where U is the set of generalized forces. Making use of the structure of T and V, the unconstrained equations of motion have the form

$$M(q)\ddot{q} + C(q, \dot{q}) + G(q) = U \tag{2}$$

where $M(q)$ is the generalized mass matrix, $C(q, \dot{q})$ is the Coriolis vector and $G(q)$ is the gravity vector.

Theorem 2.1 (Special structure of the constrained system): Given the unconstrained car model with structure as in (2) and the constraints (1), the following holds true:

(i) the dynamics of the constrained system can be written in terms of the unconstrained coordinates $q_r = [x, y, \psi]^T$ and the normal forces λ as

$$\tilde{\mathcal{M}}(q_r)\begin{bmatrix} \ddot{q}_r \\ \lambda \end{bmatrix} + \mathcal{C}(q_r, \dot{q}_r) + \mathcal{G}(q_r) = \begin{bmatrix} \mathcal{U} \\ 0 \end{bmatrix},$$

where

$$\tilde{\mathcal{M}}(q_r) = \begin{bmatrix} \mathcal{M}_{11}(q_r) & 0 \\ \mathcal{M}_{21}(q_r) & \mathcal{M}_{22}(q_r) \end{bmatrix} =$$

$$= \left[\begin{array}{ccc|cc} m & 0 & -mbs_\psi & 0 & 0 \\ 0 & m & mbc_\psi & 0 & 0 \\ -mbs_\psi & mbc_\psi & I_{zz} + mb^2 & 0 & 0 \\ \hline 0 & 0 & 0 & -1 & -1 \\ -mhc_\psi & -mhs_\psi & 0 & a+b & 0 \end{array}\right],$$

$$\mathcal{C}(q_r, \dot{q}_r) = \begin{bmatrix} \mathcal{C}_1(q_r, \dot{q}_r) \\ \mathcal{C}_2(q_r, \dot{q}_r) \end{bmatrix} = \left[\begin{array}{c} -mbc_\psi\dot{\psi}^2 \\ -mbs_\psi\dot{\psi}^2 \\ 0 \\ \hline 0 \\ (I_{xz} + mhb)\dot{\psi}^2 \end{array}\right],$$

$$\mathcal{G}(q_r) = \begin{bmatrix} \mathcal{G}_1(q_r) \\ \mathcal{G}_2(q_r) \end{bmatrix} = \left[\begin{array}{c} 0 \\ 0 \\ 0 \\ \hline -mg \\ mgb \end{array}\right],$$

$$\mathcal{U} = J_f^T(\psi) f = \begin{bmatrix} c_\psi & -s_\psi & c_\psi & -s_\psi \\ s_\psi & c_\psi & s_\psi & c_\psi \\ 0 & a+b & 0 & 0 \end{bmatrix} \begin{bmatrix} f_{fx} \\ f_{fy} \\ f_{rx} \\ f_{ry} \end{bmatrix};$$

(ii) the subsystem

$$\mathcal{M}_{11}(q_r)\ddot{q}_r + \mathcal{C}_1(q_r, \dot{q}_r) + \mathcal{G}_1(q_r) = \mathcal{U}$$

is a Lagrangian system obtained from a suitable *reduced Lagrangian* $\mathcal{L}_r(q_r)$, with normal forces

$$\mathcal{M}_{21}(q_r)\ddot{q}_r + \mathcal{M}_{22}(q_r)\lambda + \mathcal{C}_2(q_r, \dot{q}_r) + \mathcal{G}_2(q_r) = 0;$$

(iii) under the assumption that the forces f depend linearly on the normal forces, i.e.

$$\mathcal{U} = J_f^T(\psi) F \lambda = J_f^T(\psi) \begin{bmatrix} -\mu_{fx} & 0 \\ -\mu_{fy} & 0 \\ 0 & -\mu_{rx} \\ 0 & -\mu_{ry} \end{bmatrix} \lambda$$

$$= \begin{bmatrix} c_\psi\mu_{fx} - s_\psi\mu_{fy} & c_\psi\mu_{rx} - s_\psi\mu_{ry} \\ s_\psi\mu_{fx} + c_\psi\mu_{fy} & s_\psi\mu_{rx} + c_\psi\mu_{ry} \\ (a+b)\mu_{fy} & 0 \end{bmatrix} \lambda := \mathcal{M}_{12}\lambda$$

where μ_{**} are the effective tire coefficients, the car dynamics turns to be

$$\mathcal{M}(q_r)\begin{bmatrix} \ddot{q}_r \\ \lambda \end{bmatrix} + \mathcal{C}(q_r, \dot{q}_r) + \mathcal{G}(q_r) = 0$$

with

$$\mathcal{M}(q_r) = \begin{bmatrix} \mathcal{M}_{11}(q_r) & \mathcal{M}_{12}(q_r, \mu_{**}) \\ \mathcal{M}_{21}(q_r) & \mathcal{M}_{22}(q_r) \end{bmatrix}.$$

Equivalently, we can write the explicit expression

$$\begin{aligned} \ddot{q}_r &= -(\mathcal{M}_{11} + \mathcal{M}_{12}\mathcal{M}_{22}^{-1}\mathcal{M}_{21})^{-1} \\ &\quad [\mathcal{C}_1 + \mathcal{G}_1 + \mathcal{M}_{12}\mathcal{M}_{22}^{-1}(\mathcal{C}_2 + \mathcal{G}_2)] \\ \lambda &= -\mathcal{M}_{22}^{-1}(\mathcal{C}_2 + \mathcal{G}_2 + \mathcal{M}_{21}\ddot{q}_r). \end{aligned}$$

□

The proof of the theorem is omitted for the sake of space and will be provided in a forthcoming document.

We call the matrix $\mathcal{M}$ the *extended mass matrix*. An important aspect to investigate for the constrained model is the invertibility of the extended mass matrix. Differently from the standard mass matrix that is proven to be positive definite (and thus invertible), for the extended mass matrix the invertibility depends on the model and tire parameters.

Theorem 2.2 (Invertibility of the extended mass matrix): The extended mass matrix $\mathcal{M}$ is invertible if and only if

$$(\mu_{rx} - \mu_{fx}) \neq \frac{a+b}{h}. \ \square$$

The proof of the theorem is omitted for the sake of space and will be provided in a forthcoming document.

Remark 2.3: For the Pacejka's tire model and for the car/tires data provided in Appendix, it can be shown easily that the condition of Theorem 2.2 is verified. □

Next, we provide the dynamics in the body frame with respect to different coordinates. These dynamics will be helpful in the characterization of the equilibrium manifold and in the exploration strategy. First, we consider the dynamics expressed in the body frame with respect to the longitudinal and lateral accelerations seen in the body frame a_x and a_y,

$$\mathcal{M}_a \begin{bmatrix} a_x \\ a_y \\ \dot{\psi} \\ f_{fz} \\ f_{rz} \end{bmatrix} + \mathcal{C}_a + \mathcal{G}_a = 0 \tag{3}$$

with

$$\mathcal{M}_a = \begin{bmatrix} m & 0 & 0 & \mu_{fx} & \mu_{rx} \\ 0 & m & mb & \mu_{fy} & \mu_{ry} \\ 0 & mb & (I_{zz}+mb^2) & (a+b)\mu_{fy} & 0 \\ 0 & 0 & 0 & -1 & -1 \\ -mh & 0 & 0 & a+b & 0 \end{bmatrix}$$

$$\mathcal{C}_a = \begin{bmatrix} -mb\dot{\psi}^2 \\ 0 \\ 0 \\ 0 \\ (I_{xz}+mhb)\dot{\psi}^2 \end{bmatrix} \qquad \mathcal{G}_a = \begin{bmatrix} 0 \\ 0 \\ 0 \\ -mg \\ mgb \end{bmatrix}.$$

Since the dynamics do not depend on the positions x and y, and the orientation ψ, we can work on a reduced model by using the longitudinal and lateral velocities in the body frame, respectively v_x and v_y. Thus, we get

$$\mathcal{M}_v \begin{bmatrix} \dot{v}_x \\ \dot{v}_y \\ \ddot{\psi} \\ f_{fz} \\ f_{rz} \end{bmatrix} + \mathcal{C}_v + \mathcal{G}_v = 0, \tag{4}$$

where

$$\mathcal{M}_v = \begin{bmatrix} m & 0 & 0 & \mu_{fx} & \mu_{rx} \\ 0 & m & mb & \mu_{fy} & \mu_{ry} \\ 0 & mb & (I_{zz}+mb^2) & (a+b)\mu_{fy} & 0 \\ 0 & 0 & 0 & -1 & -1 \\ -mh & 0 & 0 & a+b & 0 \end{bmatrix},$$

$$\mathcal{C}_v = \begin{bmatrix} -mb\dot{\psi}^2 - mv_y\dot{\psi} \\ mv_x\dot{\psi} \\ mbv_x\dot{\psi} \\ 0 \\ (I_{xz}+mhb)\dot{\psi}^2 + mhv_y\dot{\psi} \end{bmatrix} \text{ and } \mathcal{G}_v = \begin{bmatrix} 0 \\ 0 \\ 0 \\ -mg \\ mgb \end{bmatrix}.$$

The reduced car model is a system with

3 states: v_x, v_y, $\dot{\psi}$

2 inputs: δ, κ_r.

The full model is obtained by adding three more states for the configuration variables, x, y, and ψ, with the corresponding kinematic equations.

One more version of the dynamics is obtained by choosing as states the vehicle speed v and the vehicle side-slip angle β, where $\tan\beta = v_y/v_x$. This change of coordinates is helpful to calculate the equilibrium manifold in the next section. So the equations of motion are

$$\mathcal{M}_\beta \begin{bmatrix} \dot{v} \\ \dot{\beta} \\ \ddot{\psi} \\ f_{fz} \\ f_{rz} \end{bmatrix} + \mathcal{C}_\beta + \mathcal{G}_\beta = 0 \tag{5}$$

where

$$\mathcal{M}_\beta = \begin{bmatrix} mc_\beta & -mvs_\beta & 0 & \mu_{fx} & \mu_{rx} \\ ms_\beta & mvc_\beta & mb & \mu_{fy} & \mu_{ry} \\ mbs_\beta & mbvc_\beta & (I_{zz}+mb^2) & (a+b)\mu_{fy} & 0 \\ 0 & 0 & 0 & -1 & -1 \\ -mhc_\beta & mhvs_\beta & 0 & a+b & 0 \end{bmatrix},$$

$$\mathcal{C}_\beta = \begin{bmatrix} -mv\dot{\psi}s_\beta - mb\dot{\psi}^2 \\ -mv\dot{\psi}c_\beta \\ mbv\dot{\psi}c_\beta \\ 0 \\ (I_{xz}+mhb)\dot{\psi}^2 + mhv\dot{\psi}s_\beta \end{bmatrix} \text{ and } \mathcal{G}_\beta = \begin{bmatrix} 0 \\ 0 \\ 0 \\ -mg \\ mgb \end{bmatrix}.$$

In this new set of variables, we can show that the extended mass matrix $\mathcal{M}_\beta$ is invertible if $(\mu_{rx}-\mu_{fx}) \neq \frac{p}{h}$ and $v \neq 0$.

Remark 2.4: We have a family of car models, (3), (4) and (5), that provide different insights depending on the features to investigate. In particular, we use models (3) and (5) to solve the equilibrium manifold and model (4) for trajectory exploration. □

III. Equilibrium Manifold

In this section we analyze the equilibrium manifold of the car model, i.e. the set of trajectories that can be performed by use of constant inputs. Searching for "constant" trajectories requires the solution of a set of nonlinear equations expressing the fact that all accelerations must be set to zero. We consider the model in the form (5). The equilibrium points for this system must satisfy

$$(\dot{v}, \dot{\beta}, \ddot{\psi}) = (0, 0, 0) \tag{6}$$

giving a circular path with constant speed v, yaw rate $\dot{\psi}$ and vehicle side-slip angle β. Since $\dot{\beta} = 0$, the lateral acceleration is given by $a_{lat} = v\dot{\psi}$ so that

$$\begin{aligned} a_x &= -a_{lat}\sin\beta \\ a_y &= a_{lat}\cos\beta \\ \dot{\psi} &= a_{lat}/v \end{aligned}$$

Now, referring to the dynamic model (3), we set the constraints (6) and we get the load transfer in equilibrium condition

$$-f_{fz} = mg\frac{b}{a+b} + \frac{(I_{xz}+mhb)(\frac{a_{lat}}{v})^2 + a_{lat}mh\sin\beta}{a+b}$$

$$-f_{rz} = mg\frac{a}{a+b} - \frac{(I_{xz}+mhb)(\frac{a_{lat}}{v})^2 + a_{lat}mh\sin\beta}{a+b}$$

and the following three equations:

$$\begin{aligned} ma_x - mb\dot{\psi}^2 + \mu_{fx}f_{fz} + \mu_{rx}f_{rz} &= 0 \\ ma_y + \mu_{fy}f_{fz} + \mu_{ry}f_{rz} &= 0 \\ mba_y + (a+b)\mu_{fy}f_{fz} &= 0 \end{aligned}$$

We have obtained a nonlinear system of three equations in five unknowns (v, a_{lat}, β, δ and κ_r), so that the equilibrium manifold is a two-dimensional surface. The velocity and the lateral acceleration provide an intuitive and convenient parametrization of the equilibrium manifold.

We compute the equilibrium manifold for two car models whose parameters are given in Appendix. In Figures 2 we plot the equilibrium manifold for a standard European car, while in Figures 3 we plot the equilibrium manifold for a race car, [2]. By looking at the values of β_f and β_r we can recognize two well known behaviors. If the rear side slip angle is larger than the front ($\beta_r > \beta_f$), the vehicle curves more than a kinematic steering. This is known as

oversteering. If the front side slip angle is larger than the rear ($\beta_f > \beta_r$), the vehicle follows a less curved trajectory. This is known as *understeering*.

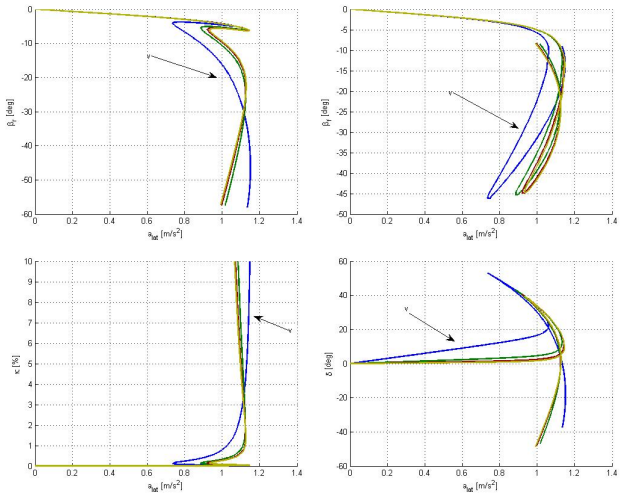

Fig. 2. Equilibrium manifold for a standard car: rear side slip, front side slip, longitudinal slip and steering angle. Specifically: $v = (10, 20, 30, 40)m/s$.

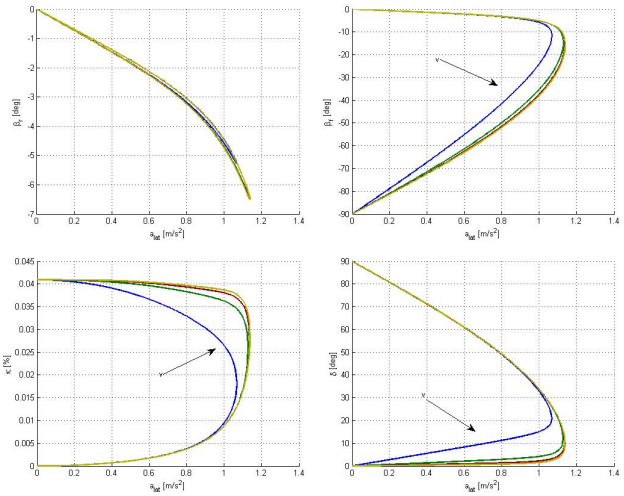

Fig. 3. Equilibrium manifold for a race car: rear side slip, front side slip, longitudinal slip and steering angle. Specifically: $v = (10, 20, 30, 40)m/s$.

IV. Trajectory exploration

In this section we describe the optimal control tools used to explore the dynamics of the car vehicle and provide numerical computations showing the effectiveness of the proposed exploration strategy.

A. Projection operator Newton method for the optimization of trajectory functionals

We are interested in studying the set of trajectories of a nonlinear system described by ordinary differential equations on $\mathbb{R}^n$ with inputs on $\mathbb{R}^m$. A trajectory of the system is a curve $\eta = (x(\cdot), u(\cdot))$ defined on $L_\infty[0, T)$ such that

$$\dot{x}(t) = f(x(t), u(t)) \tag{7}$$

for all $t \in [0, T]$, where $f : \mathbb{R}^n \times \mathbb{R}^m \longrightarrow \mathbb{R}^n$ and $f \in \mathcal{C}^r$ with $0 \leq r \leq \infty$.

To facilitate the local exploration of trajectories of the nonlinear system, we use the Projection Operator Newton method developed in [10], see also [11]. We take a trajectory tracking approach, defining a projection operator that maps a state-control curve (e.g., a desired curve) onto the trajectory manifold. Specifically, the time varying trajectory tracking control law

$$\begin{aligned} \dot{x} =& f(x, u), \qquad x(0) = x_0, \\ u(t) =& \mu(t) + K(t)(\alpha(t) - x(t)) \end{aligned}$$

defines the projection operator $\mathcal{P} : \xi = (\alpha(\cdot), \mu(\cdot)) \mapsto \eta = (x(\cdot), u(\cdot))$, taking the curve $\xi = (\alpha(\cdot), \mu(\cdot))$ to the trajectory $\eta = (x(\cdot), u(\cdot))$. Now, we consider the following problem: find a trajectory of the system (7) that minimizes the L_2 distance from a desired curve $\xi_{des} = (x_{des}(\cdot), u_{des}(\cdot))$. Formally, given the positive definite symmetric matrices Q, R and P_1, we want to minimize the cost functional:

$$\begin{aligned} h(\xi) = \frac{1}{2} \int_0^T \|x(\tau) - x_{des}(\tau)\|_Q^2 + \|u(\tau) - u_{des}(\tau)\|_R^2 d\tau \\ + \frac{1}{2} \|x(T) - x_{des}(T)\|_{P_1}^2 \end{aligned}$$

In compact notation we can write the following constrained optimization problem $\min_{\xi \in \mathcal{T}} h(\xi) = \min_{\xi = \mathcal{P}(\xi)} h(\xi)$, where $\mathcal{T}$ is the manifold of bounded trajectories $(x(\cdot), u(\cdot))$ on $[0, T]$. Defining the function $g(\xi) := h(\mathcal{P}(\xi))$, the optimal control problem can be equivalently reformulated as $\min_{\xi \in \mathcal{T}} h(\xi) \iff \min_\xi g(\xi)$. Thus, the constrained optimization problem is converted into an unconstrained one. Here, the weights Q, R and P_1 are design variables that reflect the relative importance of certain components of the desired trajectory. Furthermore, these weights should also be chosen in a manner that reflects dynamic capabilities of the system. The minimization of the trajectory functional is accomplished by iterating over the following algorithm, where ξ_i indicates the current trajectory, starting with an initial trajectory ξ_0.

Algorithm (projection operator Newton method)
Given initial trajectory $\xi_0 \in \mathcal{T}$
For $i = 0, 1, 2...$

design K defining $\mathcal{P}$ about ξ_i
search direction

$$\zeta_i = \arg \min_{\zeta \in T_{\xi_i} \mathcal{T}} Dg(\xi_i) \cdot \zeta + \frac{1}{2} D^2 g(\xi_i)(\zeta, \zeta)$$

step size $\gamma_i = \arg \min_{\gamma \in (0,1]} g(\xi + \gamma \zeta_i)$;

project $\xi_{i+1} = \mathcal{P}(\xi_i + \gamma_i \zeta_i)$.

end

B. Aggressive turn from a real testing track

We present an example of trajectory exploration of the car model. The desired trajectory consists of following a turn (from a real testing track) at constant speed. In particular, we choose a desired speed ($25m/s$) that in a portion of the turn gives a lateral acceleration exceeding the tire limits. At

the begininning the vehicle is in the center of the road with yaw angle and rate set to zero and initial speed of $25m/s$. The algorithm converges in twenty-one iterations. In Figures 4 the optimal trajectory compared with the desired one is shown.

In the first straight portion, the vehicle decelerates and moves on the left of the track to gain the most favorable position to enter the turn. In the second portion the car is in full deceleration to face the right bend. The sharp deceleration leads to a strong load transfer onto the front. Because of the strong load transfer, the rear must have a high side slip angle (in order to generate the required lateral forces), see Figures 5. We can notice that the vehicle is slightly oversteered since the front side slip angle is smaller than the back one. Then the car starts the exit from the bend. With the decreasing of the centrifugal force, the lateral forces on the tires decrease, so that the longitudinal ones can increase. Thus, the car accelerates in order to regain the desired speed.

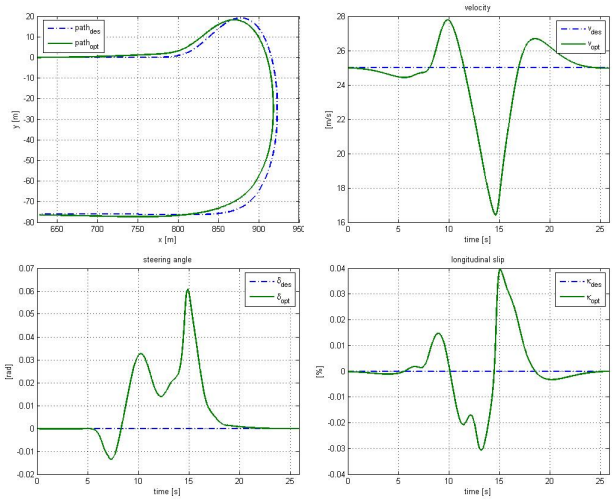

Fig. 4. Optimal trajectory on a real curve track: track, velocity, steering angle and longitudinal slip. Specifically: desidered velocity constant at $25m/s$, desidered lateral acceleration (maximum value inside the curve) at $1.568g$.

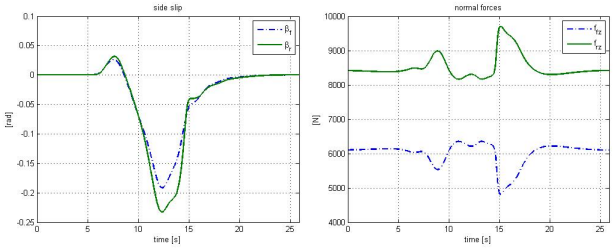

Fig. 5. Optimal trajectory on a real curve track: the front/rear side slip (left), and front/rear normal force (right).

V. Conclusions

In this paper we studied the problem of modeling and exploring the dynamics of a single-track rigid car model that takes into account tire models and load transfer. We developed a new model of car that (to our knowledge) has never been studied in the literature. Starting from the bicycle model we introduced the load transfer phenomenon by explicitly imposing the holonomic constraints for the contact with the ground. This model shows many of the interesting dynamic effects of a real car. Then we characterized the equilibrium manifold of the rigid car model and analyzed how it changes with respect to suitable parameters. Finally, we provided a set of strategies, based on nonlinear optimal control techniques, to explore the trajectories of the car model. We provided numerical computations showing the effectiveness of the exploration strategy on a slice of a real testing track.

References

[1] W. F. Milliken, D. L. Milliken, *Race car vehicle dynamics*, SAE, 1995.
[2] G. Genta, *Meccanica dell'autoveicolo*, Levrotto & Bella, 2000.
[3] H. B. Pacejka, *Tire and Vehicle dynamics*, Butterworth Heinemann, 2002.
[4] Thomas D. Gillespie, *Fundamentals of Vehicle Dynamics*, SAE, Warrendale, 1992.
[5] J. Y. Wong, *Theory of ground vehicles*, John Wiley & Sons, 2001.
[6] E. Bakker, L. Nyborg, H. B. Pacejka, *Tyre Modelling for Use in Vehicle Dynamics Studies*, SAE, 1987.
[7] R. S. Sharp, S. Evangelou, D. J. N. Limebeer, *Advances in the Modelling of Motorcycle Dynamics*, Kluwer Academic Publishers, 2004.
[8] S. Evangelou, *The Control and Stability Analysis of Two-wheeled Road Vehicles*, Imperial College London, 2003.
[9] P. MacMillin, J. Hauser, *Development and Exploration of a Rigid Motorcycle Model*, CDC, 2009.
[10] J. Hauser, *A projection operator approach to optimization of trajectory functionals*, IFAC World Congress, 2002.
[11] J. Hauser, D. G. Meyer, *The trajectory manifold of a nonlinear control system*, CDC, 1998.
[12] A. Saccon, *Maneuver Regulation of Nonlinear Systems: The Challenge of Motorcycle Control*, Ph.D. Thesis, Padova, 2006
[13] K. Manssouri, *Integrated Motion Control of an Overactuated Vehicle*, Master Thesis, Eindhoven, 2004

Appendix

These parameters are based on those given in Genta, [2].

	standard car	*race car*
$m\ [kg]$	1150	1480
$a\ [m]$	1.064	1.421
$b\ [m]$	1.596	1.029
$h\ [m]$	0.57	0.42
$I_{zz}\ [kgm^2]$	1850	1950
$I_{xz}\ [kgm^2]$	-120	-50

While, the parameters of the wheels are based on those given in Evangelou, [8].

	front	*rear*
μ_x	1.381	1.355
c_x	1.61	1.61
b_x	11.696	11.919
e_x	0.0263	0.0263
$c_{x\beta}$	1.1231	1.1231
r_{bx1}	13.476	13.476
r_{bx2}	11.354	11.354
μ_y	1.3	1.3
c_y	0.833	0.9
b_y	15.418	11.478
e_y	-1.256	-2.223
$c_{y\kappa}$	1.0533	1.0533
r_{by1}	7.7856	7.7856
r_{by2}	8.1697	8.1697